Published in final edited form as:
J Mol Cell Cardiol. 2014 January ; 66: 83–93. doi:10.1016/j.yjmcc.2013.11.001.

PKA catalytic subunit compartmentation regulates contractile and hypertrophic responses to β-adrenergic signaling

Jason H. Yang, Ph.D, **Renata K. Polanowska-Grabowska, Ph.D**, **Jeffrey S. Smith, B.S**, **Charles W. Shields IV, B.S**, and **Jeffrey J. Saucerman, Ph.D**
Department of Biomedical Engineering, University of Virginia; Robert M. Berne Cardiovascular Research Center, University of Virginia

Abstract

β-adrenergic signaling is spatiotemporally heterogeneous in the cardiac myocyte, conferring exquisite control to sympathetic stimulation. Such heterogeneity drives the formation of protein kinase A (PKA) signaling microdomains, which regulate Ca^{2+} handling and contractility. Here, we test the hypothesis that the nucleus independently comprises a PKA signaling microdomain regulating myocyte hypertrophy. Spatially-targeted FRET reporters for PKA activity identified slower PKA activation and lower isoproterenol sensitivity in the nucleus (t_{50} = 10.60±0.68 min; EC_{50} = 89.00 nmol/L) than in the cytosol (t_{50} = 3.71±0.25 min; EC_{50} = 1.22 nmol/L). These differences were not explained by cAMP or AKAP-based compartmentation. A computational model of cytosolic and nuclear PKA activity was developed and predicted that differences in nuclear PKA dynamics and magnitude are regulated by slow PKA catalytic subunit diffusion, while differences in isoproterenol sensitivity are regulated by nuclear expression of protein kinase inhibitor (PKI). These were validated by FRET and immunofluorescence. The model also predicted differential phosphorylation of PKA substrates regulating cell contractility and hypertrophy. Ca^{2+} and cell hypertrophy measurements validated these predictions and identified higher isoproterenol sensitivity for contractile enhancements (EC_{50} = 1.84 nmol/L) over cell hypertrophy (EC_{50} = 85.88 nmol/L). Over-expression of spatially targeted PKA catalytic subunit to the cytosol or nucleus enhanced contractile and hypertrophic responses, respectively. We conclude that restricted PKA catalytic subunit diffusion is an important PKA compartmentation mechanism and the nucleus comprises a novel PKA signaling microdomain, insulating hypertrophic from contractile β-adrenergic signaling responses.

1. Introduction

In healthy humans, the body responds to deficiencies in blood flow by releasing catecholamines and acutely increasing contractility in the heart [1]. However, chronic sympathetic stimulation can initiate cardiac remodeling events such as hypertrophy and fibrosis, driving the heart failure phenotype [2]. Over time, these effects can further

Corresponding Author: Jeffrey J. Saucerman (jsaucerman@virginia.edu).
Present Address: Department of Biomedical Engineering, PO Box 800759, Charlottesville, VA 22908, United States of America, Phone: (434) 924-5095, Fax: (434) 982-3870

Disclosures
None.

stimulate catecholamine release and drive further electromechanical dysfunction and sudden cardiac death.

Many groups, including our own, have observed spatiotemporal heterogeneity in β-adrenergic signaling in the cardiac myocyte, suggesting compartmentation may underlie β-adrenergic signaling specificity [3–6]. Common to these studies is the hypothesis that spatially heterogeneous cAMP gradients [5–7] or A-kinase anchoring proteins (AKAPs) [8, 9] restrict the activity of PKA catalytic subunit to small local signaling microdomains. Here, we test a complementary hypothesis that compartmentation of PKA catalytic subunit itself may also regulate β-adrenergic signaling.

We combined live-cell imaging with computational modeling and high-throughput hypertrophy imaging to examine nuclear PKA compartmentation in primary cardiac myocytes. We observed differences in cytosolic and nuclear PKA signaling dynamics and sensitivity to isoproterenol (ISO), which were not explained by cAMP or AKAP compartmentation. Using a computational model, we inferred roles for rate-limiting PKA catalytic subunit diffusion and nuclear PKI expression for regulating nuclear PKA signaling, which are consistent with subsequent validation experiments. By over-expressing PKA catalytic subunit in either the cytosol or nucleus, we found nuclear PKA compartmentation may differentially regulate cardiac myocyte contractility and hypertrophy.

2. Materials and Methods

2.1 Cardiomyocyte Isolation and Culture

Neonatal rat ventricular myocytes were isolated from the hearts of 1–2 day old Sprague-Dawley rats using the Cellutron Neomyt Cardiomyocyte Isolation kit (Cellutron Life Technologies, Baltimore, MD) and cultured on Surecoat-treated 35 mm glass-bottom dishes (MatTek, Ashland, MA), Surecoat-treated 6-well plates or CellBIND-coated 96-well plates (Corning, Corning, NY) as described previously [10]. All procedures were performed in accordance with the Guide for the Care and Use of Laboratory Animals published by the National Institutes of Health and approved by the University of Virginia Institutional Animal Care and Use Committee.

2.2 Spatially Targeted PKA Over-Expression

mCherry-labeled PKA catalytic subunits containing a C-terminal nuclear export sequence (-NES) or nuclear localization sequence (-NLS) were constructed by ligating the PKA-NES or PKA-NLS segments from CMV-EGFP-PKA-NES or CMV-EGFP-PKA-NLS [11] into the mCherry-C1 expression vector (Clontech, Mountain View, CA) at the BSPEI/BamHI restriction sites. Transfection was performed using Lipofectamine 2000 (Invitrogen, Carlsbad, CA).

2.3 Ca^{2+} Imaging

Two days after isolation, myocytes cultured in 35 mm glass-bottom dishes were transferred to serum-free media for 24 hours. One day later, cultured myocytes were loaded with Fluo-4 AM (Invitrogen, Carlsbad, CA). Loaded myocytes were paced at 1 Hz using the C-Pace EP Culture Pacer (IonOptix, Milton, MA) and stimulated with isoproterenol (ISO; Tocris, Minneapolis, MN) dissolved in Tyrode's solution. Paced myocytes were imaged on an IX-81 inverted microscope (Olympus, Center Valley, PA) with a Digital CCD C9300-221 camera (Hamamatsu, Bridgewater, NJ) at 10 Hz using MetaMorph® Automation and Image Analysis Software (Molecular Devices, Sunnyvale, CA). Cells were segmented in ImageJ (National Institutes of Health, Bethesda, MA) and analyzed in MATLAB (Mathworks, Natick, MA).

2.4 Hypertrophy Measurements

Two days after isolation, myocytes cultured in 96-well plates were transfected with cTnT-EGFP plasmid [12] using Lipofectamine 2000. Expressing myocytes were imaged on an Olympus IX-81 inverted microscope with an automated stage (Prior Scientific, Rockland, MA) and an Orca-AG CCD camera (Hamamatsu, Bridgewater, NJ) using IPLab (Scanalytics, Fairfax, VA), as described previously [10]. Images were segmented automatically and analyzed in MATLAB using custom automated image processing algorithms.

2.5 FRET Imaging

Two days after isolation, myocytes cultured in 35 mm glass-bottom dishes were transfected with CMV-AKAR-NES, CMV-AKAR-NLS, CMV-ICUE-NES or CMV-ICUE-NLS [13, 14] plasmid using Lipofectamine 2000. Expressing myocytes were imaged on an Olympus IX-81 inverted microscope with an Orca-AG CCD camera using IPLab. Tyrode's Solution was used as a negative control at the beginning of each experiment and a cocktail of 50 μmol/L forskolin (FSK; Tocris, Minneapolis, MN) and 100 μmol/L 3-isobytl-1-methylxanthine (IBMX; Sigma-Aldrich, St. Louis, MO) was used as a positive control at the end of each experiment. FRET computations were performed in MATLAB using the PFRET algorithm [15]. Cells were segmented in ImageJ and FRET responses were normalized to positive and negative controls in MATLAB. Where indicated, myocytes were pre-incubated in Tyrode's solution with 20 μg/mL wheat germ agglutinin (WGA; Sigma-Aldrich, St. Louis, MO) before stimulation with either ISO or FSK+IBMX.

2.6 Computational Modeling

Nuclear PKA activity was modeled by modifying our previously published ordinary differential equation implementation of cardiac β-adrenergic signaling [16, 17] to include nuclear PKA transport, PKI transport and AKAR expression/phosphorylation (Supplement). The expanded model was implemented in MATLAB and constrained to parameters estimated from published literature. The final model contained 34 state variables and 104 parameters. Before each simulation, new initial conditions were generated by running the model to steady-state without ISO stimulation.

2.7 Immunofluorescence

Two days after isolation, myocytes cultured in 35 mm glass-bottom dishes were fixed in 4% paraformaldehyde (Fisher Scientific, Pittsburgh, PA) and permeabilized with 0.2% Triton X-100 (MP Biomedicals, Solon, OH). PKIα was detected using rabbit polyclonal anti-PKIα primary antibodies (Lifespan Biosciences, Seattle WA) and goat anti-rabbit secondary antibodies conjugated with Alexa488 (Invitrogen, Carlsbad, CA). Following washout, cells were imaged on an Olympus IX-81 inverted microscope with an Orca-AG CCD camera using IPLab and analyzed in ImageJ.

2.8 Western Blots

Two days after isolation, myocytes cultured in 6-well plates were treated with ISO for 30 minutes and lysed with Pierce RIPA Buffer (Thermo Scientific, Rockford, IL) supplemented with Complete Protease Inhibitor Cocktail Tablets (Roche, Indianapolis, IN) and Halt Phosphatase Inhibitor Cocktail (Thermo Scientific). To quantify nuclear PKA catalytic subunit accumulation, cells were fractionated into nuclear and cytosolic fractions using NE-PER Nuclear Protein Extraction Kit (Thermo Scientific) supplemented with Protease Inhibitor Cocktail. Samples were electrophoresed on 10% SDS-PAGE gels and then electrotransferred onto PVDF membranes at 100 V for 1 hour. The membranes were probed with affinity-purified rabbit polyclonal antibodies specific for PKA Cα (Cell Signaling

Technology, Danvers, MA). Mouse anti-fibrillarin antibodies (Abcam, Cambridge, England) were used as nuclear loading controls, while mouse anti-α-tubulin antibodies (LI-COR Biosciences, Lincoln, NE) were used as cytosolic loading controls. To quantify CREB and phospholamban (PLB) phosphorylation, samples were resolved on 15% SDS-polyacrylamide gels by electrophoresis and then transferred to Immobilon-FL PVDF membranes (Millipore, Billerica, MA). Blots were probed using rabbit anti-phospho-PLB (Ser16/Thr17) or rabbit anti-phospho-CREB (Ser133) antibodies (Cell Signaling Technology). Mouse anti-α-tubulin antibodies (LI-COR Biosciences) were used as protein loading controls. Phosphorylated PLB and CREB were visualized using goat anti-rabbit IRDye800 CW secondary antibodies, while α-tubulin was detected using goat anti-mouse IRDye680 CW secondary antibodies (LI-COR Biosciences). All membranes were scanned on a LI-COR Odyssey scanner. Signal intensities for each experiment were quantified using Image Studio Lite (LI-COR Biosciences). All bands were normalized to their respective loading controls.

2.9 Statistics

All statistical analyses were performed using Prism 5.0 (GraphPad, La Jolla, CA). EC_{50}s for ISO-stimulated Ca^{2+} enhancements, hypertrophy, FRET responses and PLB and CREB phosphorylation were fitted to a variable slope dose-response curve. Unpaired *t*-tests were performed on ICUE and AKAR t_{50}s. A one-way ANOVA was performed on Western blot measurments of nuclear PKA catalytic subunit enrichment. Non-parametric Mann-Whitney tests were performed on hypertrophy measurements. Hypertrophy measurements are reported as median±standard error of median. All other statistics are reported as mean ±standard error of mean.

3. Results

3.1 PKA Activity is Compartmented and Differentially Sensitive to ISO

We recently showed that the nucleus comprises a PKA signaling microdomain in HEK293 cells [18]. To determine if PKA signaling is similarly compartmented in cardiac myocytes, we expressed PKA-specific FRET reporters targeted to either the cytosol (AKAR-NES) or nucleus (AKAR-NLS) in neonatal rat ventricular myocytes (Fig. 1A). Treating these myocytes with ISO, we identified significant differences between cytosolic and nuclear PKA in both dynamics and ISO sensitivity. Stimulation with 1 μmol/L ISO induced almost 3-fold faster PKA responses in the cytosol (t_{50} = 3.71±0.25 min) than in the nucleus (t_{50} = 10.60±0.68 min) (Fig. 1B). Subsequent treatment with 10 μmol/L propranolol (PRO), a non-selective beta blocker, reversed PKA activity (faster in the cytosol than the nucleus) (Fig. 1B). Stimulating over a range of ISO concentrations, we observed more sensitive PKA activity in the cytosol (EC_{50} = 1.22 nmol/L) than in the nucleus (EC_{50} = 89.00 nmol/L) (Fig. 1C, 1D). Differences in cytosolic and nuclear PKA sensitivity were surprising because differential regulation of PKA substrate phosphorylation is thought to be regulated by AKAPs, which directly localize PKA substrates to PKA holoenzyme [19]. However, no endogenous AKAPs are expected to have affinity for AKAR-NES or AKAR-NLS.

3.2 Nuclear PKA Compartmentation is Not Explained by cAMP Compartmentation

cAMP compartmentation by phosphodiesterases (PDEs) is thought to be an important regulator of PKA compartmentation; and we have previously shown nuclear PKA activity in HEK293 cells may be regulated by a nuclear PDE-PKA-AKAP complex [18]. To test if cAMP compartmentation similarly explains these differences in cytosolic and nuclear PKA dynamics in cardiomyocytes, we treated myocytes with 50 μmol/L forskolin (FSK), an adenylyl cyclase activator, and 100 μmol/L 3-isobutyl-1-methylxanthine (IBMX), a non-selective phosphodiesterase inhibitor. In myocytes expressing cAMP-specific FRET

reporters targeted to either the cytosol (ICUE-NES) or nucleus (ICUE-NLS), combined FSK +IBMX treatment induced a rapid and robust cAMP response in both the cytosol and nucleus (cytosol: t_{50} = 1.62±0.13 min; nucleus: t_{50} = 0.77±0.05 min) (Fig. 2A, 2C). In contrast, FSK+IBMX induced a 12-fold slower response in the nucleus (t_{50} = 7.15±0.70 min) than in the cytosol (t_{50} = 0.59±0.02 min) (Fig. 2B, 2C). These results suggest differences in cytosolic and nuclear PKA dynamics are not primarily due to cAMP compartmentation.

Pre-incubating myocytes with 50 μmol/L Ht31, an A-kinase anchoring protein (AKAP) inhibitor, did not accelerate or enhance nuclear PKA dynamics induced by ISO (Fig. 2D, S1) as we had previously seen in HEK293 cells [18]. Ht31 pre-treatment significantly reduced the peak amplitude of AKAR-NES responses to 1 μmol/L ISO (Fig. S1), consistent with previous measurements of troponin I and myosin binding protein C phosphorylation [20]. However, we did not observe a significant effect on either the peak amplitude or the kinetics of AKAR-NLS phosphorylation (Fig. 2E, 2F), suggesting that AKAPs are not the major mechanism limiting nuclear PKA activity.

3.3 A Computational Model for Nuclear PKA Activity

Computational models have contributed significantly to the understanding of cardiac signaling networks [21]. We previously modeled the β_1-adrenergic signaling pathway [16] and its actions on cytosolic rat [22] and mouse myocyte physiology [17]. To better understand nuclear PKA compartmentation quantitatively, we introduced a nuclear compartment to these models (Fig. 3A; Supplement). We assumed that activated PKA catalytic subunit (C) passively diffuses into the nucleus via nuclear pore complexes [23], where it may phosphorylate nuclear PKA substrates such as cAMP response element binding protein (CREB) [24]. In turn, phospho-CREB is dephosphorylated by protein phosphatase 2A (PP2A) [25]. Protein kinase inhibitor (PKI) limits this process by competitively inhibiting free PKA catalytic subunit [26]. AKAR-NES and AKAR-NLS were modeled as in previous studies [27]. When the 4 unknown PKA/PKI nuclear transport parameters were fitted to the experimental data in Fig. 1, simulated AKAR-NES and AKAR-NLS responses were similar to measured responses in both kinetics (Fig. 3B) and ISO sensitivity (Fig. 3C).

3.4 Nuclear PKA Activity Dynamics are Rate-Limited by PKA Catalytic Subunit Diffusion

PKA catalytic subunit is 38 kDa, while cAMP is a small molecule with a molecular mass of 329.2 Da. Nuclear pore complexes have a cargo threshold of ~40 kDa [28]. We therefore hypothesized that nuclear PKA activation is rate-limited by PKA catalytic subunit diffusion rather than cAMP diffusion, consistent with observations that nuclear PKA accumulation is slow following cytosolic catalytic subunit microinjection [23]. Model simulations predicted that further decreases in PKA nuclear import would decrease the steady-state magnitude of nuclear PKA activity, suggesting nuclear PKA activity is rate-limited by PKA catalytic subunit diffusion (Fig. 4A). Restricting nuclear transport to 1% ablated the simulated AKAR-NLS response to 1 μmol/L ISO. We tested this prediction experimentally by pre-incubating myocytes expressing AKAR-NLS with 20 μg/mL wheat germ agglutinin (WGA) for 30 min, which may directly inhibit nuclear transport by binding nuclear pores [29]. Consistent with model predictions, myocytes pre-incubated with WGA displayed significantly attenuated AKAR-NLS responses with 1 μmol/L ISO (Fig. 4B). In contrast to the AKAR-NLS measurements, pre-treatment with WGA did not significantly inhibit the magnitude of AKAR-NES responses, indicating intact cytosolic β-adrenergic signaling under these conditions (Fig. 4C). Moreover, WGA did not significantly alter phosphorylation kinetics for AKAR-NES (t_{50} = 1.01±0.12 min), indicating a specific effect for WGA pre-treatment on nuclear PKA activity (Fig. 4D), as predicted by the model (Fig.

4A). We confirmed these FRET measurements by performing western blots for PKA catalytic subunit on nuclear fractions of myocytes with and without WGA pre-incubation. WGA pre-incubation blocked nuclear translocation of PKA catalytic subunit by either ISO stimulation or treatment with FSK and IBMX (Fig. 4E, 4F), but did not alter catalytic subunit expression in whole cell lysates (Fig. S2). These observations support the hypothesis that nuclear PKA activity in myocytes is not regulated by nuclear cAMP compartmentation but rather by direct compartmentation of PKA catalytic subunit.

3.5 Biased PKIα Expression May Underlie Differential ISO Sensitivity of PKA

The lower ISO sensitivity for nuclear PKA activity (Fig. 1D) suggests the nucleus may constitute a PKA signaling microdomain distinct from the cytosol. Substrate phosphorylation represents a delicate balance between local kinase and phosphatase activity. If cAMP is not rate-limiting nuclear PKA activity (Fig. 2A, 2B), then differences between nuclear and cytosolic AKAR phosphorylation are likely explained by either greater nuclear phosphatase activity or decreased nuclear PKA availability. In addition to limited PKA catalytic subunit nuclear import, nuclear PKA availability may also be modulated by competitive inhibition and export of PKA catalytic subunit by PKI [26, 30]. To better understand if the differential ISO sensitivity of nuclear and cytosolic AKAR were quantitatively explained by nuclear phosphatase activity or by nuclear PKA availability, we simulated perturbations to these mechanisms in our model and then experimentally validated corollaries to each hypothesis.

We first tested the hypothesis that nuclear phosphatases could explain the lower ISO-sensitivity in the nucleus compared to the cytosol. The baseline model assumes similar phosphatase concentrations for the cytosol and nucleus. As expected, simulated increases in nuclear phosphatase expression decreased the predicted magnitude of AKAR-NLS phosphorylation, indicating nuclear phosphatases are important regulators of nuclear PKA substrates (Fig. 5A). Yet nuclear phosphatase inhibition did not increase sensitivity of nuclear PKA activity to ISO stimulation (Fig. 5B), in contrast to intuitive expectations based on simpler Goldbeter-Koshland kinetics [31] (due to the additional actions of PKI, see Fig. S3). We validated this model prediction experimentally by first pre-incubating myocytes with 10 nmol/L Calyculin A (an inhibitor of PP1 and PP2A phosphatases), and then measuring AKAR-NLS responses to 10 nmol/L or 10 μmol/L ISO, which produced very different AKAR-NLS responses in control cells (Fig. 1C, 1D). We chose this concentration as Calyculin A has an IC_{50} of ~1 nmol/L for PP2A and ~2 nmol/L for PP1 [32]. Consistent with model predictions, pre-treatment with 10 nmol/L Calyculin A did not alter the ISO sensitivity for AKAR-NLS (Fig. 5C). Moreover, stimulation with Calyculin A alone revealed similar steady-state phosphorylation levels for both AKAR-NES and AKAR-NLS (Fig. S4). Together, these results suggest nuclear phosphatases are not the major factor underlying the differential ISO sensitivity of PKA activity between cytosol and nucleus.

We then tested the hypothesis that nuclear PKI could be responsible for the differences in nuclear and cytosolic ISO sensitivity. When developing the model (Section 3.3), we found a bias towards nuclear PKI expression was necessary to quantitatively reproduce the reduced AKAR-NLS sensitivity to ISO (Fig. 1D). When cytosolic and nuclear PKI expression were set to equal values, the model predicted similar ISO sensitivity between cytosolic and nuclear PKA (Fig. 5D). To test the model-predicted nuclear bias of PKI, we immunolabeled fixed myocytes with anti-PKIα antibodies and found nearly exclusive nuclear PKIα expression (Fig. 5E). Together, these results suggest differences in cytosolic and nuclear ISO sensitivity may be due to a nuclear bias in PKIα expression (limiting the availability of PKA catalytic subunit) rather than a bias in nuclear phosphatase activity.

3.6 PKA Compartmentation May Differentially Elicit Contractile and Hypertrophic Responses

We next hypothesized that cytosolic-nuclear PKA compartmentation may be relevant for regulating β-adrenergic signaling responses of endogenous PKA substrates. To test this, we modeled the phosphorylation of well-characterized PKA substrates residing in the cytosol (PLB, phospholamban) and nucleus (CREB, cAMP response element binding protein). The model predicted reduced p-CREB ISO sensitivity (EC_{50} = 31.46 nmol/L) compared to p-PLB (EC_{50} = 4.95 nmol/L) (Fig. 6A), consistent with the reduced ISO sensitivities of nuclear PKA activity (Fig. 1D). We validated this model prediction by Western blotting steady-state PLB and CREB phosphorylation over a range of ISO concentrations (Fig. 6B, S5; p-PLB EC_{50} = 0.58 nmol/L; p-CREB EC_{50} = 52.68 nmol/L).

Because PLB and CREB regulate Ca^{2+} transients and hypertrophy, respectively [33], we hypothesized that stimulated enhancements to Ca^{2+} transients and hypertrophy might also exhibit differential ISO sensitivity. To test this hypothesis experimentally, we treated myocytes with ISO and measured enhancements to Ca^{2+} transients and cell size. At 1 μmol/L ISO, steady-state Ca^{2+} transient amplitudes exhibited a 63.5±15.1% enhancement (Fig. 6C). Similarly, 1 μmol/L ISO induced a 24.2±3.5% increase in cell size after 24 hours (Fig. 6D). We observed Ca^{2+} handling to be much more sensitive than hypertrophy to lower doses of ISO (EC_{50} = 1.84 nmol/L vs. EC_{50} = 85.88 nmol/L) (Fig. 6E), similar to ISO sensitivity differences for cytosolic/nuclear PKA activity (Fig. 1D) and the simulated and measured differences in PLB and CREB ISO sensitivity (Fig. 6A, 6B). While PLB and CREB are not the exclusive mediators of β-adrenergic stimulated contractility and hypertrophy, these results suggest cytosolic and nuclear PKA activity may differentially elicit contractile and hypertrophic responses.

To test the functional consequences of perturbed cytosolic/nuclear PKA compartmentation, we over-expressed mCherry-labeled PKA catalytic subunit targeted to either the cytosol (PKA-NES) or nucleus (PKA-NLS) (Fig. 7A). Under 1 Hz pacing, we observed larger baseline Ca^{2+} transients in PKA-NES myocytes over either mCherry or PKA-NLS myocytes (Fig. 7B, 7C), complemented by ablated sensitivity to 1 μmol/L ISO (Fig. 7D). These suggest PKA-NES over-expression was saturating the phosphorylation of contractility-relevant PKA substrates, while PKA-NLS over-expression had little effect on these targets. In contrast, PKA-NLS myocytes were hypertrophied (1401±38 μm^2; n = 1324 cells) over both mCherry (1213±37 μm^2; n = 944 cells) and PKA-NES myocytes (1291±44 μm^2; n = 945 cells) (Fig. 7E). These enhancements were specific to the activity of PKA, as incubation with 10 μmol/L H-89 blocked this hypertrophy (Fig. S6). While these results cannot exclude the documented hypertrophic contributions of cytosolic AKAP-bound PKA [34] or other signaling pathways downstream of PKA [35], our data overall suggests cytosolic PKA primarily enhances contractility under β-adrenergic stimulation, while enhanced nuclear PKA primarily contributes to hypertrophy.

4. Discussion

4.1 PKA Compartmentation in β-Adrenergic Signaling

Numerous groups have now investigated mechanisms regulating spatiotemporal heterogeneity in cardiac β-adrenergic signaling [3, 36]. While some have focused on receptor localization [7, 37, 38], receptor subtype [39, 40] or PKA regulatory subunit subtype [41], PDEs [6, 42] and AKAPs [8, 9] have prominently risen as key regulatory mechanisms of compartmented β-adrenergic signaling. Common to these studies is the underlying hypothesis that β-adrenergic signaling responses are managed by phosphorylation of PKA substrates local to PKA holoenzyme, which become activated by spatially heterogeneous cAMP gradients. While PKA catalytic subunits released from RIα

regulatory subunits may not diffuse far from RIα, PKA catalytic subunit is capable of diffusing away from RIIα upon cAMP elevation [43, 44]. Here, we report a complementary view to the local-activation/local-action view for PKA signaling, whereby PKA can diffuse from the cytosol into the nucleus to exert functionally relevant, distal actions in the nucleus of cardiac myocytes. This view is further supported by observations that type II PKA can diffuse great distances, navigating complex geometries in neurons [45].

Several studies implicate AKAPs in PKA-dependent regulation of hypertrophy [34]. For example both mAKAP and AKAP-Lbc promote hypertrophy [46, 47], with outer nuclear membrane and peri-nuclear targeting, respectively [20, 47, 48]. Moreover, we have previously shown that nuclear PKA dynamics in HEK293 cells may be explained by nuclear PDE4D-PKA-AKAP complexes [18]. This inference was based on accelerated nuclear PKA dynamics following PDE inhibition by IBMX or AKAP disruption by Ht31. In contrast, here in cardiac myocytes we observed slow nuclear PKA activity despite rapid nuclear cAMP accumulation by FSK/IBMX and did not observe accelerated nuclear PKA dynamics with Ht31. These data suggest resident intra-nuclear pools of PKA holoenzyme (waiting to be activated by cAMP) are limited in cardiac myocytes. Thus, mAKAP and AKAP-Lbc may facilitate hypertrophy by releasing catalytic subunit near nuclear pores, and our results suggest nuclear PKA activity dynamics are rate-limited by slow diffusion of free PKA catalytic subunit [23], similar to findings by others in neurons [49].

Our observation that cytosolic and nuclear PKA activities exhibit different sensitivities to β-adrenergic stimulation suggests the nucleus comprises an independent PKA signaling microdomain. While nuclear phosphatases clearly regulate the magnitude of nuclear PKA substrate phosphorylation, our model analysis suggests that the observed differences in ISO sensitivity are better explained by spatially heterogeneous PKI expression than by differential phosphatase activity. This inference is corroborated by a history of observations that PKI can specifically inhibit nuclear PKA activity by competitively inhibiting free PKA catalytic subunit and by inducing active export of PKA catalytic subunit from the nucleus [26]. In particular PKIα overexpression has been shown to decrease the expression of PKA-regulated genes in neurons [30] and recent studies over-expressing PKIα's inhibitory domain demonstrate protection from ISO-stimulated cardiac hypertrophy in transgenic mice [50], though the over-expressed PKI in those experiments did not localize specifically to the nucleus. While these results suggest PKI may limit nuclear PKA activity in a mechanism analogous to PDE-regulation of cAMP, we cannot exclude the possibility that nuclear PKA activity is regulated by other proteins. For instance, the PKIα knockout mouse exhibits compensatory expression of PKA regulatory subunit RIα, which similarly sequesters and buffers PKA catalytic subunit and limits the expression of PKA-regulated genes in skeletal muscle [51]. As PKI is relatively unstudied in the heart, further work will be necessary to evaluate how it regulates PKA compartmentation.

4.2 Relevance to Cardiac Physiology and Disease

We found that cytosolic-nuclear PKA compartmentation regulates endogenous substrates and cardiac myocyte functions, which may affect cardiac physiology in several ways. First, differences in cytosolic and nuclear PKA sensitivity to ISO suggest such compartmentation may insulate myocytes from inducing hypertrophic growth when β-ARs are engaged to enhance contractility. This has therapeutic implications as treatment with β-blockers attenuates cardiac remodeling during heart failure, but also sensitizes patients to bradycardia and low blood pressure [52]. If chronotropic and inotropic responses can be separated from hypertrophic responses by cytosolic-nuclear compartmentation, nuclear PKA inhibition may be an attractive gene therapy target over enhancements to excitation-contraction coupling or antagonism of β-adrenergic signaling alone [53]. Studies by others also implicate an important role for cytosolic-nuclear PKA compartmentation in cell survival in spiral

ganglion neurons [11] and actin organization in PC12 cells [54]. Future work will be necessary to characterize other nuclear PKA-dependent effects in the heart.

Second, nuclear PKA activity is an order of magnitude slower than cytosolic PKA activity. These results suggest a second mode of insulation for PKA-stimulated transcriptional activity: the requirement for sustained β-AR stimulation. Thus, while contractile responses may be activated by small and acute sympathetic activity, hypertrophic responses associated with pathologic cardiac remodeling may require large and chronic sympathetic activity. These could in part explain how daily engagement of the *fight-or-flight* response does not drive the heart toward a failing phenotype, while chronically elevated sympathetic activity may prime the heart for rapid deterioration [55]. While further *in vivo* studies will be necessary to confirm these findings, the current work suggests PKA catalytic subunit compartmentation may contribute to the bifurcation between physiologic β-adrenergic signaling and pathologic β-adrenergic remodeling.

4.3 β-Adrenergic Signaling-Stimulated Hypertrophy

While it is well-recognized that β-adrenergic stimulation is sufficient for stimulating cardiac hypertrophy, hypertrophy signaling is complex [56] and the specific mechanisms for these observations remain unclear. Transgenic over-expression studies indicate that β_1-AR [57], $G_{s\alpha}$ [58] or PKA [59] are all sufficient for inducing hypertrophy and heart failure *in vivo*. Other studies have shown β-adrenergic signaling stimulates hypertrophy in a PKA-independent manner via cAMP activation of Epac [60], though this view has recently been challenged by studies showing hearts from mice overexpressing PKI are protected against ISO-stimulated hypertrophy [50]. Moreover, as PKA directly enhances Ca^{2+} signaling, PKA-mediated hypertrophy may be managed by enhanced CaMKII [61] or calcineurin/NFAT [62] signaling. Still others suggest PKA may actually inhibit hypertrophy via HDAC5 phosphorylation [63] or HDAC4 proteolysis [64]. Here, we observe hypertrophy in myocytes over-expressing nuclear PKA catalytic subunit. These results are not mutually exclusive with findings by others, but support a hypothesis that chronic β-adrenergic stimulation can stimulate PKA catalytic subunit to escape local control by PDE or AKAP compartmentation mechanisms and distally initiate cardiac remodeling events in the nucleus. Future work will need to clarify the direct role of nuclear PKA activity in cardiac hypertrophy.

4.4 Limitations and Considerations

We have taken a multi-disciplinary approach to investigate PKA catalytic subunit compartmentation, integrating live-cell imaging experiments from neonatal rat ventricular myocytes with computational modeling. While seminal studies in cardiac β-adrenergic compartmentation were performed using neonatal rat myocytes [5, 27, 41, 65–67], care must be taken in interpreting the role of PKA catalytic subunit compartmentation in human heart failure. We chose myocyte cell hypertrophy as an approximation for ventricular hypertrophy in the intact heart. While these *in vitro* findings alone do not prove that nuclear PKA activity critically drives pathologic cardiac hypertrophy in human pathology, these results do support the hypothesis that PKA activity in the cytosol and nucleus exerts different cardiac behaviors.

Carefully constrained computational models can provide significant insight into the mechanics of cell signaling and provide inspiration for new experimental studies [21]. Here, we carefully assembled and validated our model from published biochemical data and used the model as a hypothesis-generating inference tool to investigate mechanisms underlying PKA catalytic subunit compartmentation. We minimized bias in these simulations by first making prospective modeling predictions and then following with subsequent experimental

validations. By performing our analysis using these standards, we built confidence that the computational model adequately represented the biology and that the model predictions were reasonable hypotheses for testing.

5. Conclusions

In summary, we provide direct evidence that PKA catalytic subunit forms functionally relevant, diffusion-limited signaling compartments. We show PKA activity in the nucleus is slower and less sensitive than cytosolic PKA activity to β-AR agonists. These differences in dynamics are rate-limited by PKA diffusion rather than cAMP compartmentation. Moreover, differences in signaling sensitivity appear prescribed by nuclear PKI rather than nuclear phosphatase activity. Elevated cytosolic PKA activity directly enhanced Ca^{2+} transients, but had little effect on myocyte hypertrophy. Conversely, elevated nuclear PKA activity induced myocyte hypertrophy, but had no effect on Ca^{2+} transients. Together, these findings suggest PKA catalytic subunit compartmentation may help explain how chronic, but not acute, β-adrenergic stimulation may initiate cardiac remodeling and drive the progression of heart failure.

Supplementary Material

Refer to Web version on PubMed Central for supplementary material.

Acknowledgments

The authors thank Lindsay McLellan (University of Virginia) for her assistance in performing myocyte isolations and Dr. Jeffrey Holmes (University of Virginia) for helpful discussions. The authors also thank Dr. Brent French (University of Virginia) for sharing cTnT-EGFP plasmid; Dr. Jin Zhang (Johns Hopkins Medical Institutes) for sharing AKAR3-NES, AKAR3-NLS, ICUE3-NES and ICUE3-NLS plasmids; and Dr. Steven Green (University of Iowa) for sharing EGFP-PKA-NES and EGFP-PKA-NLS plasmids.

Funding Sources

This work was supported by NIH R01 HL094476 to J.J.S., the American Heart Association (0830470N to J.J.S. and 0715283U to J.H.Y) and the Biotechnology Training Program (NIH T32 GM08715 to J.H.Y.).

Abbreviations

β-AR	β-adrenergic receptor
AKAP	A-kinase anchoring protein
CREB	cAMP response element binding protein
FSK	forskolin
IBMX	3-isobytl-1-methylxanthine
ISO	isoproterenol
NES	nuclear export sequence
NLS	nuclear localization sequence
PDE	phosphodiesterase
PKA	protein kinase A
PKI	protein kinase inhibitor
PP2A	protein phosphatase 2A

WGA wheat germ agglutinin

References

1. Katz, AM. Physiology of the heart. 5. Philadelphia, PA: Wolters Kluwer Health/Lippincott Williams & Wilkins Health; 2011.
2. Katz AM. The “modern” view of heart failure: how did we get here? Circ Heart Fail. 2008; 1:63–71. [PubMed: 19808272]
3. Xiang YK. Compartmentalization of beta-adrenergic signals in cardiomyocytes. Circ Res. 2011; 109:231–44. [PubMed: 21737818]
4. Steinberg SF, Brunton LL. Compartmentation of G protein-coupled signaling pathways in cardiac myocytes. Annu Rev Pharmacol Toxicol. 2001; 41:751–73. [PubMed: 11264475]
5. Zaccolo M, Pozzan T. Discrete microdomains with high concentration of cAMP in stimulated rat neonatal cardiac myocytes. Science. 2002; 295:1711–5. [PubMed: 11872839]
6. Fischmeister R, Castro LR, Abi-Gerges A, Rochais F, Jurevicius J, Leroy J, et al. Compartmentation of cyclic nucleotide signaling in the heart: the role of cyclic nucleotide phosphodiesterases. Circ Res. 2006; 99:816–28. [PubMed: 17038651]
7. Nikolaev VO, Bunemann M, Schmitteckert E, Lohse MJ, Engelhardt S. Cyclic AMP imaging in adult cardiac myocytes reveals far-reaching beta1-adrenergic but locally confined beta2-adrenergic receptor-mediated signaling. Circ Res. 2006; 99:1084–91. [PubMed: 17038640]
8. Diviani D, Dodge-Kafka KL, Li J, Kapiloff MS. A-kinase anchoring proteins: scaffolding proteins in the heart. Am J Physiol Heart Circ Physiol. 2011; 301:H1742–53. [PubMed: 21856912]
9. McConnachie G, Langeberg LK, Scott JD. AKAP signaling complexes: getting to the heart of the matter. Trends Mol Med. 2006; 12:317–23. [PubMed: 16809066]
10. Ryall KA, Saucerman JJ. Automated imaging reveals a concentration dependent delay in reversibility of cardiac myocyte hypertrophy. J Mol Cell Cardiol. 2012; 53:282–90. [PubMed: 22575844]
11. Bok J, Zha XM, Cho YS, Green SH. An extranuclear locus of cAMP-dependent protein kinase action is necessary and sufficient for promotion of spiral ganglion neuronal survival by cAMP. J Neurosci. 2003; 23:777–87. [PubMed: 12574406]
12. Prasad KM, Xu Y, Yang Z, Acton ST, French BA. Robust cardiomyocyte-specific gene expression following systemic injection of AAV: in vivo gene delivery follows a Poisson distribution. Gene Ther. 2011; 18:43–52. [PubMed: 20703310]
13. Allen MD, Zhang J. Subcellular dynamics of protein kinase A activity visualized by FRET-based reporters. Biochem Biophys Res Commun. 2006; 348:716–21. [PubMed: 16895723]
14. DiPilato LM, Zhang J. The role of membrane microdomains in shaping beta2-adrenergic receptor-mediated cAMP dynamics. Mol Biosyst. 2009; 5:832–7. [PubMed: 19603118]
15. Chen Y, Periasamy A. Intensity range based quantitative FRET data analysis to localize protein molecules in live cell nuclei. J Fluoresc. 2006; 16:95–104. [PubMed: 16397825]
16. Saucerman JJ, Brunton LL, Michailova AP, McCulloch AD. Modeling beta-adrenergic control of cardiac myocyte contractility in silico. J Biol Chem. 2003; 278:47997–8003. [PubMed: 12972422]
17. Yang JH, Saucerman JJ. Phospholemman is a negative feed-forward regulator of Ca(2+) in beta-adrenergic signaling, accelerating beta-adrenergic inotropy. J Mol Cell Cardiol. 2012
18. Sample V, DiPilato LM, Yang JH, Ni Q, Saucerman JJ, Zhang J. Regulation of nuclear PKA revealed by spatiotemporal manipulation of cyclic AMP. Nat Chem Biol. 2012; 8:375–82. [PubMed: 22366721]
19. Greenwald EC, Saucerman JJ. Bigger, better, faster: principles and models of AKAP anchoring protein signaling. J Cardiovasc Pharmacol. 2011; 58:462–9. [PubMed: 21562426]
20. Fink MA, Zakhary DR, Mackey JA, Desnoyer RW, Apperson-Hansen C, Damron DS, et al. AKAP-mediated targeting of protein kinase a regulates contractility in cardiac myocytes. Circulation research. 2001; 88:291–7. [PubMed: 11179196]

21. Yang JH, Saucerman JJ. Computational models reduce complexity and accelerate insight into cardiac signaling networks. Circ Res. 2011; 108:85–97. [PubMed: 21212391]
22. Saucerman JJ, McCulloch AD. Mechanistic systems models of cell signaling networks: a case study of myocyte adrenergic regulation. Prog Biophys Mol Biol. 2004; 85:261–78. [PubMed: 15142747]
23. Harootunian AT, Adams SR, Wen W, Meinkoth JL, Taylor SS, Tsien RY. Movement of the free catalytic subunit of cAMP-dependent protein kinase into and out of the nucleus can be explained by diffusion. Mol Biol Cell. 1993; 4:993–1002. [PubMed: 8298196]
24. Goldspink PH, Russell B. The cAMP response element binding protein is expressed and phosphorylated in cardiac myocytes. Circ Res. 1994; 74:1042–9. [PubMed: 8187274]
25. Wadzinski BE, Wheat WH, Jaspers S, Peruski LF Jr, Lickteig RL, Johnson GL, et al. Nuclear protein phosphatase 2A dephosphorylates protein kinase A-phosphorylated CREB and regulates CREB transcriptional stimulation. Mol Cell Biol. 1993; 13:2822–34. [PubMed: 8386317]
26. Dalton GD, Dewey WL. Protein kinase inhibitor peptide (PKI): a family of endogenous neuropeptides that modulate neuronal cAMP-dependent protein kinase function. Neuropeptides. 2006; 40:23–34. [PubMed: 16442618]
27. Saucerman JJ, Zhang J, Martin JC, Peng LX, Stenbit AE, Tsien RY, et al. Systems analysis of PKA-mediated phosphorylation gradients in live cardiac myocytes. Proc Natl Acad Sci U S A. 2006; 103:12923–8. [PubMed: 16905651]
28. Bagley S, Goldberg MW, Cronshaw JM, Rutherford S, Allen TD. The nuclear pore complex. J Cell Sci. 2000; 113 (Pt 22):3885–6. [PubMed: 11058073]
29. Finlay DR, Newmeyer DD, Price TM, Forbes DJ. Inhibition of in vitro nuclear transport by a lectin that binds to nuclear pores. J Cell Biol. 1987; 104:189–200. [PubMed: 3805121]
30. Repunte-Canonigo V, Lutjens R, van der Stap LD, Sanna PP. Increased expression of protein kinase A inhibitor alpha (PKI-alpha) and decreased PKA-regulated genes in chronic intermittent alcohol exposure. Brain Res. 2007; 1138:48–56. [PubMed: 17270154]
31. Goldbeter A, Koshland DE Jr. An amplified sensitivity arising from covalent modification in biological systems. Proceedings of the National Academy of Sciences of the United States of America. 1981; 78:6840–4. [PubMed: 6947258]
32. Ishihara H, Martin BL, Brautigan DL, Karaki H, Ozaki H, Kato Y, et al. Calyculin A and okadaic acid: inhibitors of protein phosphatase activity. Biochemical and biophysical research communications. 1989; 159:871–7. [PubMed: 2539153]
33. Saucerman JJ, McCulloch AD. Cardiac beta-adrenergic signaling: from subcellular microdomains to heart failure. Ann N Y Acad Sci. 2006; 1080:348–61. [PubMed: 17132794]
34. Blant A, Czubryt MP. Promotion and inhibition of cardiac hypertrophy by A-kinase anchor proteins. Can J Physiol Pharmacol. 2012; 90:1161–70. [PubMed: 22856508]
35. Ryall KA, Holland DO, Delaney KA, Kraeutler MJ, Parker AJ, Saucerman JJ. Network reconstruction and systems analysis of cardiac myocyte hypertrophy signaling. The Journal of biological chemistry. 2012; 287:42259–68. [PubMed: 23091058]
36. Fu Q, Chen X, Xiang YK. Compartmentalization of beta-adrenergic signals in cardiomyocytes. Trends Cardiovasc Med. 2013; 23:250–6. [PubMed: 23528751]
37. Nikolaev VO, Moshkov A, Lyon AR, Miragoli M, Novak P, Paur H, et al. Beta2-adrenergic receptor redistribution in heart failure changes cAMP compartmentation. Science. 2010; 327:1653–7. [PubMed: 20185685]
38. Xiang Y, Rybin VO, Steinberg SF, Kobilka B. Caveolar localization dictates physiologic signaling of beta 2-adrenoceptors in neonatal cardiac myocytes. J Biol Chem. 2002; 277:34280–6. [PubMed: 12097322]
39. Soto D, De Arcangelis V, Zhang J, Xiang Y. Dynamic protein kinase a activities induced by beta-adrenoceptors dictate signaling propagation for substrate phosphorylation and myocyte contraction. Circ Res. 2009; 104:770–9. [PubMed: 19213958]
40. Woo AY, Xiao RP. beta-Adrenergic receptor subtype signaling in heart: From bench to bedside. Acta Pharmacol Sin. 2012; 33:335–41. [PubMed: 22286918]

41. Di Benedetto G, Zoccarato A, Lissandron V, Terrin A, Li X, Houslay MD, et al. Protein kinase A type I and type II define distinct intracellular signaling compartments. Circ Res. 2008; 103:836–44. [PubMed: 18757829]
42. Zaccolo M, Movsesian MA. cAMP and cGMP signaling cross-talk: role of phosphodiesterases and implications for cardiac pathophysiology. Circ Res. 2007; 100:1569–78. [PubMed: 17556670]
43. Martin BR, Deerinck TJ, Ellisman MH, Taylor SS, Tsien RY. Isoform-specific PKA dynamics revealed by dye-triggered aggregation and DAKAP1alpha-mediated localization in living cells. Chem Biol. 2007; 14:1031–42. [PubMed: 17884635]
44. Manni S, Mauban JH, Ward CW, Bond M. Phosphorylation of the cAMP-dependent protein kinase (PKA) regulatory subunit modulates PKA-AKAP interaction, substrate phosphorylation, and calcium signaling in cardiac cells. The Journal of biological chemistry. 2008; 283:24145–54. [PubMed: 18550536]
45. Zhong H, Sia GM, Sato TR, Gray NW, Mao T, Khuchua Z, et al. Subcellular dynamics of type II PKA in neurons. Neuron. 2009; 62:363–74. [PubMed: 19447092]
46. Pare GC, Bauman AL, McHenry M, Michel JJ, Dodge-Kafka KL, Kapiloff MS. The mAKAP complex participates in the induction of cardiac myocyte hypertrophy by adrenergic receptor signaling. Journal of cell science. 2005; 118:5637–46. [PubMed: 16306226]
47. Carnegie GK, Soughayer J, Smith FD, Pedroja BS, Zhang F, Diviani D, et al. AKAP-Lbc mobilizes a cardiac hypertrophy signaling pathway. Mol Cell. 2008; 32:169–79. [PubMed: 18951085]
48. Kapiloff MS, Schillace RV, Westphal AM, Scott JD. mAKAP: an A-kinase anchoring protein targeted to the nuclear membrane of differentiated myocytes. Journal of cell science. 1999; 112 (Pt 16):2725–36. [PubMed: 10413680]
49. Gervasi N, Hepp R, Tricoire L, Zhang J, Lambolez B, Paupardin-Tritsch D, et al. Dynamics of protein kinase A signaling at the membrane, in the cytosol, and in the nucleus of neurons in mouse brain slices. The Journal of neuroscience : the official journal of the Society for Neuroscience. 2007; 27:2744–50. [PubMed: 17360896]
50. Zhang X, Szeto C, Gao E, Tang M, Jin J, Fu Q, et al. Cardiotoxic and cardioprotective features of chronic beta-adrenergic signaling. Circulation research. 2013; 112:498–509. [PubMed: 23104882]
51. Gangolli EA, Belyamani M, Muchinsky S, Narula A, Burton KA, McKnight GS, et al. Deficient gene expression in protein kinase inhibitor alpha Null mutant mice. Molecular and cellular biology. 2000; 20:3442–8. [PubMed: 10779334]
52. Klapholz M. Beta-blocker use for the stages of heart failure. Mayo Clin Proc. 2009; 84:718–29. [PubMed: 19648389]
53. Tilemann L, Ishikawa K, Weber T, Hajjar RJ. Gene therapy for heart failure. Circ Res. 2012; 110:777–93. [PubMed: 22383712]
54. Gerits N, Mikalsen T, Kostenko S, Shiryaev A, Johannessen M, Moens U. Modulation of F-actin rearrangement by the cyclic AMP/cAMP-dependent protein kinase (PKA) pathway is mediated by MAPK-activated protein kinase 5 and requires PKA-induced nuclear export of MK5. J Biol Chem. 2007; 282:37232–43. [PubMed: 17947239]
55. Eschenhagen T. Beta-adrenergic signaling in heart failure-adapt or die. Nat Med. 2008; 14:485–7. [PubMed: 18463653]
56. Heineke J, Molkentin JD. Regulation of cardiac hypertrophy by intracellular signalling pathways. Nat Rev Mol Cell Biol. 2006; 7:589–600. [PubMed: 16936699]
57. Engelhardt S, Hein L, Wiesmann F, Lohse MJ. Progressive hypertrophy and heart failure in beta1-adrenergic receptor transgenic mice. Proc Natl Acad Sci U S A. 1999; 96:7059–64. [PubMed: 10359838]
58. Gaudin C, Ishikawa Y, Wight DC, Mahdavi V, Nadal-Ginard B, Wagner TE, et al. Overexpression of Gs alpha protein in the hearts of transgenic mice. J Clin Invest. 1995; 95:1676–83. [PubMed: 7706476]
59. Antos CL, Frey N, Marx SO, Reiken S, Gaburjakova M, Richardson JA, et al. Dilated cardiomyopathy and sudden death resulting from constitutive activation of protein kinase a. Circ Res. 2001; 89:997–1004. [PubMed: 11717156]

60. Morel E, Marcantoni A, Gastineau M, Birkedal R, Rochais F, Garnier A, et al. cAMP-binding protein Epac induces cardiomyocyte hypertrophy. Circ Res. 2005; 97:1296–304. [PubMed: 16269655]

61. Mishra S, Ling H, Grimm M, Zhang T, Bers DM, Brown JH. Cardiac hypertrophy and heart failure development through Gq and CaM kinase II signaling. J Cardiovasc Pharmacol. 2010; 56:598–603. [PubMed: 20531218]

62. Houser SR, Molkentin JD. Does contractile Ca2+ control calcineurin-NFAT signaling and pathological hypertrophy in cardiac myocytes? Sci Signal. 2008; 1:pe31. [PubMed: 18577756]

63. Chang CW, Lee L, Yu D, Dao K, Bossuyt J, Bers DM. Acute beta-adrenergic activation triggers nuclear import of histone deacetylase 5 and delays G(q)-induced transcriptional activation. J Biol Chem. 2013; 288:192–204. [PubMed: 23161540]

64. Backs J, Worst BC, Lehmann LH, Patrick DM, Jebessa Z, Kreusser MM, et al. Selective repression of MEF2 activity by PKA-dependent proteolysis of HDAC4. J Cell Biol. 2011; 195:403–15. [PubMed: 22042619]

65. Mongillo M, McSorley T, Evellin S, Sood A, Lissandron V, Terrin A, et al. Fluorescence resonance energy transfer-based analysis of cAMP dynamics in live neonatal rat cardiac myocytes reveals distinct functions of compartmentalized phosphodiesterases. Circ Res. 2004; 95:67–75. [PubMed: 15178638]

66. Kapiloff MS, Piggott LA, Sadana R, Li J, Heredia LA, Henson E, et al. An adenylyl cyclase-mAKAPbeta signaling complex regulates cAMP levels in cardiac myocytes. J Biol Chem. 2009; 284:23540–6. [PubMed: 19574217]

67. Liu S, Zhang J, Xiang YK. FRET-based direct detection of dynamic protein kinase A activity on the sarcoplasmic reticulum in cardiomyocytes. Biochem Biophys Res Commun. 2011; 404:581–6. [PubMed: 21130738]

Highlights

- Nuclear PKA is slower and less sensitive to ISO than cytosolic PKA in cardiac myocytes
- Nuclear PKA compartmentation is not due to cAMP compartmentation
- Nuclear PKA dynamics are regulated by passive nuclear transport
- Nuclear PKA ISO sensitivity may be regulated by nucleus-biased PKI expression
- PKA compartmentation may differentially regulate contractility and hypertrophy

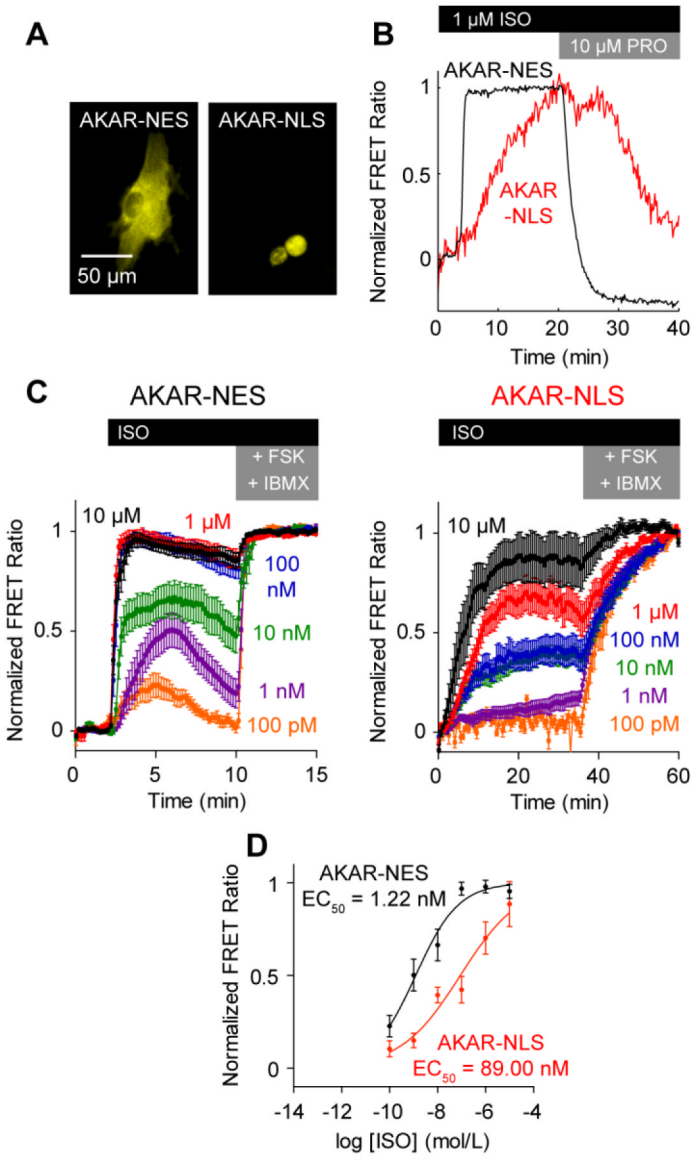

Fig. 1.

Cytosolic PKA and nuclear PKA activities differ in dynamics and ISO sensitivity. A, Representative expression of cytosolic AKAR-NES and nuclear AKAR-NLS FRET reporters. B, Representative responses to 1 μmol/L ISO and 10 μmol/L PRO. Nuclear PKA activity is slower than cytosolic PKA activity. C, Averaged AKAR-NES and AKAR-NLS responses to ISO stimulation, normalized to 50 μmol/L FSK + 100 μmol/L IBMX (n ≥ 9 cells each). D, Cytosolic PKA activity exhibits a higher ISO sensitivity than nuclear PKA activity.

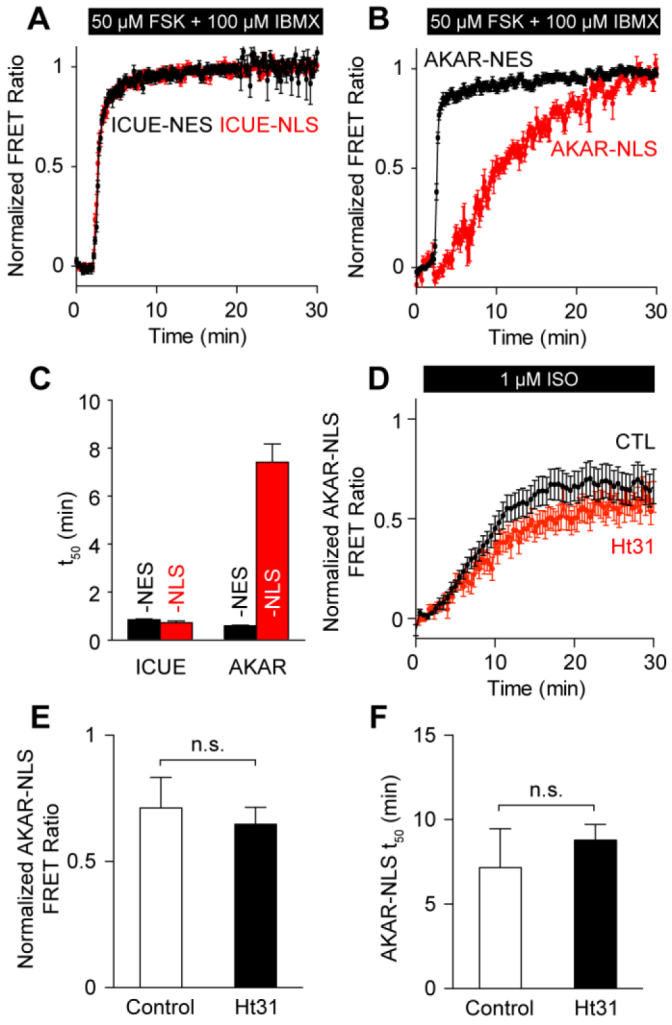

Fig. 2.

Distinct nuclear PKA dynamics are not explained by cAMP compartmentation or AKAPs. A, Mean cytosolic ICUE-NES (n = 12 cells) and nuclear ICUE-NLS (n = 12 cells) responses to 50 μmol/L FSK + 100 μmol/L IBMX. B, Mean cytosolic AKAR-NES (n = 9 cells) and nuclear AKAR-NLS (n = 11 cells) responses to 50 μmol/L FSK + 100 μmol/L IBMX. C, cAMP accumulation occurs rapidly in both the cytosol and nucleus, while PKA activation occurs rapidly in the cytosol only. D, AKAP disruption by 50 μmol/L Ht31 does not significantly perturb AKAR-NLS responses (n = 16 cells). 1 μmol/L ISO responses from Ht31 treated cells are similar to those from untreated cells in both peak magnitude (E) and kinetics (F).

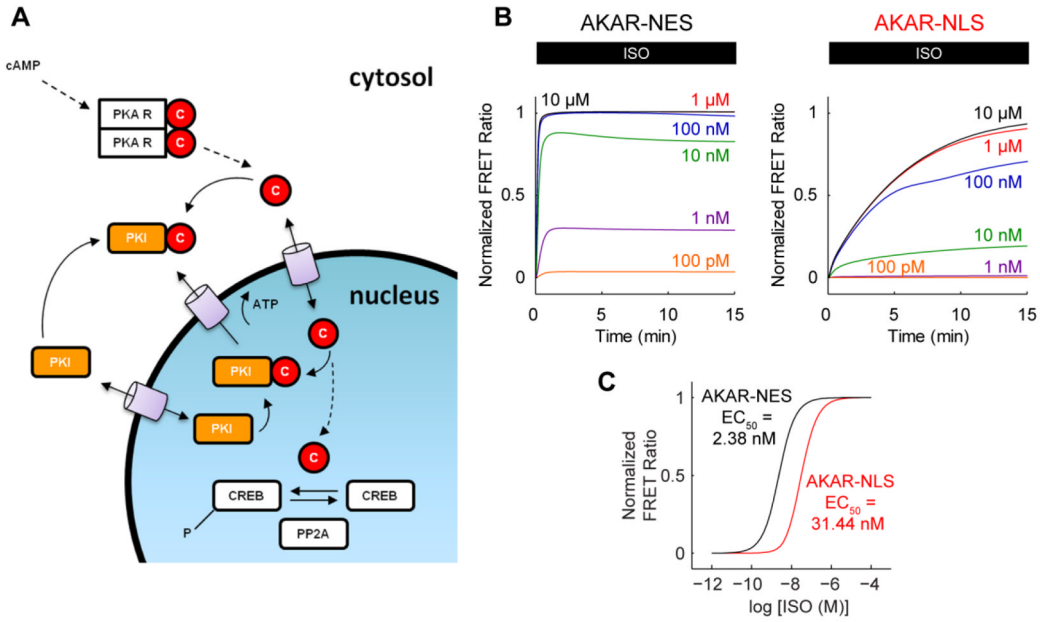

Fig. 3.

A computational model for nuclear PKA compartmentation in cardiac myocytes. A, Schematic for nuclear PKA compartment extension to our previously published β-adrenergic signaling models. B, Model-predicted AKAR-NES and AKAR-NLS responses to ISO stimulation. C, Model-predicted AKARNES and AKAR-NLS ISO sensitivities. Model responses are qualitatively similar to experimentally measured differences in dynamics and ISO sensitivity.

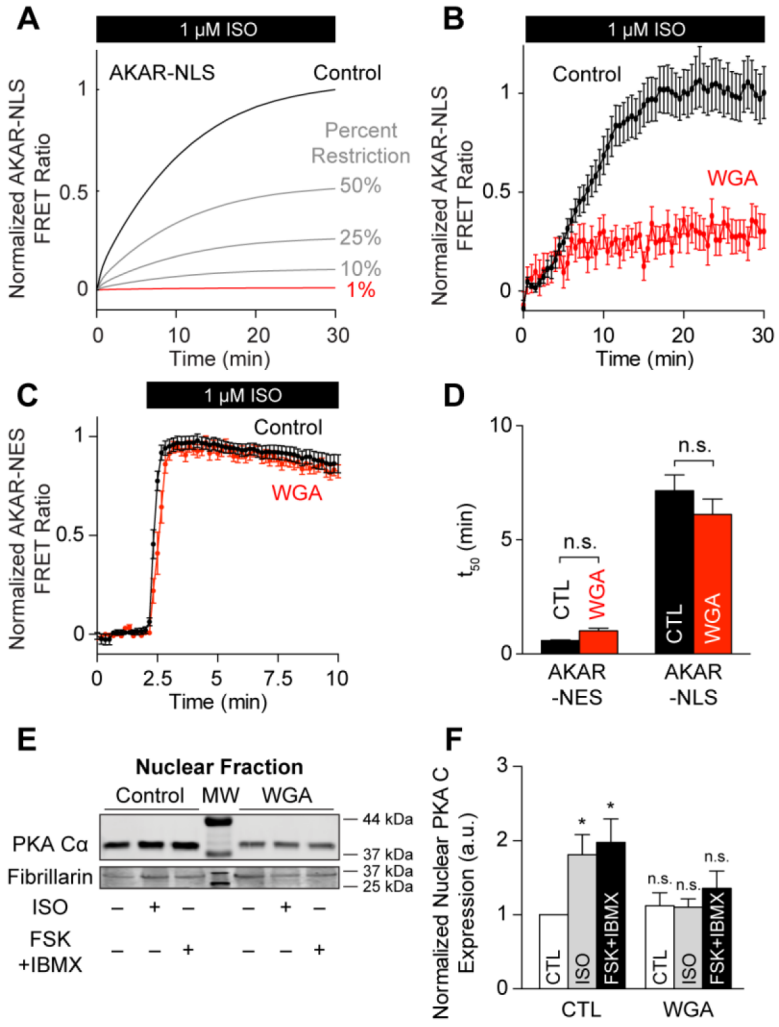

Fig. 4.

Passive diffusion rate-limits nuclear PKA activity. A, Model-predicted AKAR-NLS responses to 1 μmol/L ISO stimulation. Reducing PKA's nuclear diffusion rate shrinks the rate and magnitude of AKAR-NLS phosphorylation. B, Experimental validation for model prediction. Mean AKAR-NLS responses to 1 μmol/L ISO stimulation following 30 min pre-incubation with 20 μg/mL WGA (n = 22 cells). C, WGA pre-incubation does not inhibit cytosolic AKAR-NES responses to 1 μmol/L ISO (n = 16 cells). D, WGA pre-treatment does not change the t_{50} for either AKAR-NES or AKAR-NLS responses to 1 μmol/L ISO. E, Representative Western blot for PKA catalytic subunit accumulation in nuclear fractions of control and WGA-treated myocytes. F, WGA pre-incubation inhibits nuclear PKA accumulation after either ISO or FSK+IBMX treatment (n = 5 replicates; *: $p \leq 0.05$ vs. untreated control).

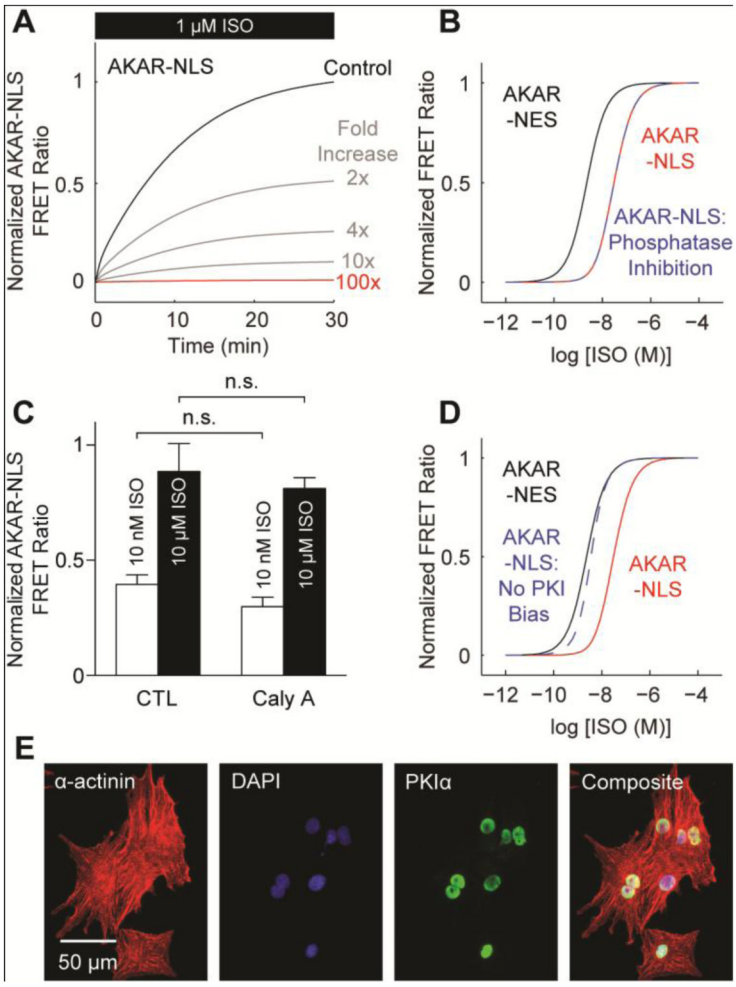

Fig 5.

Biased PKIα expression may reduce nuclear PKA sensitivity to ISO stimulation. A, Simulated AKAR-NLS responses to 1 μmol/L ISO with increasing nuclear phosphatase expression. B, Model predicts nuclear phosphatase inhibition does not recover AKAR-NLS's ISO sensitivity. C, Experimental validation for model simulations. Pre-treatment with 10 nmol/L Calyculin A does not alter nuclear AKAR-NLS sensitivity to ISO ($n \geq 9$ cells each). D, Model predicts nuclear PKA ISO sensitivity requires biased PKI expression. E, Immunofluorescence labeling with anti-PKIα antibodies identify nearly exclusive nuclear PKIα expression.

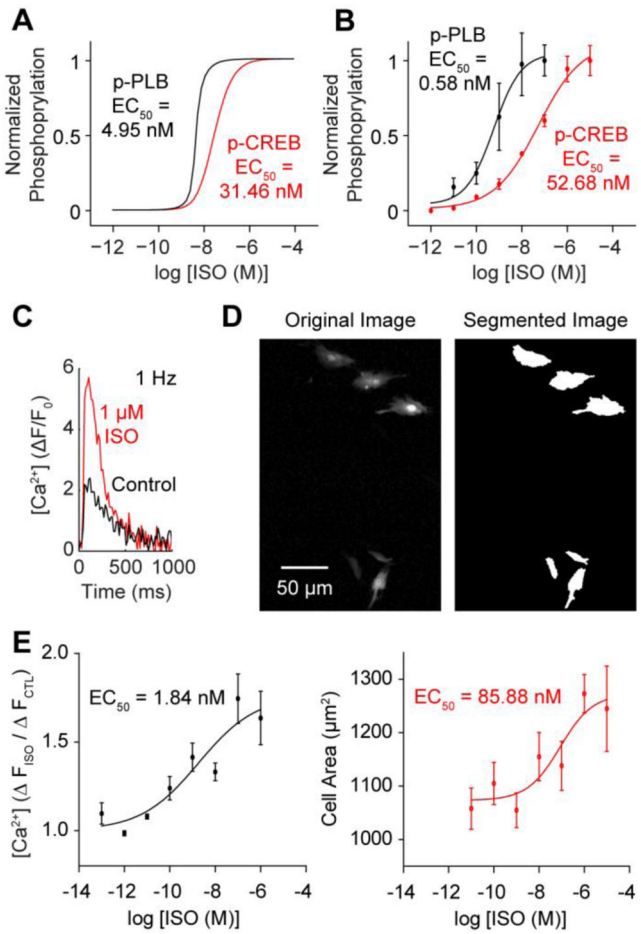

Fig. 6.

PKA compartmentation drives differential activation of PKA substrates associated with contractility and hypertrophy. A, Model prediction for phosphorylated PLB and CREB sensitivity to ISO. p-PLB and p-CREB EC_{50}s parallel cytosolic and nuclear PKA EC_{50}s, respectively. B, Western blot analysis indicates PLB phosphorylation is significantly more sensitive to ISO than CREB phosphorylation (n = 3 experiments each). C, Representative Ca^{2+} transient measurements from control and 1 μmol/L ISO-stimulated myocytes paced at 1 Hz. D, Representative automated cell segmentations from myocytes cultured in 1 μmol/L ISO for 24 hours. E, ISO-stimulated Ca^{2+} enhancements exhibit high ISO sensitivity ($n \geq 3$ experiments per ISO concentration), while 24 hour myocyte hypertrophy responses are less sensitive to ISO (n > 250 cells per ISO concentration).

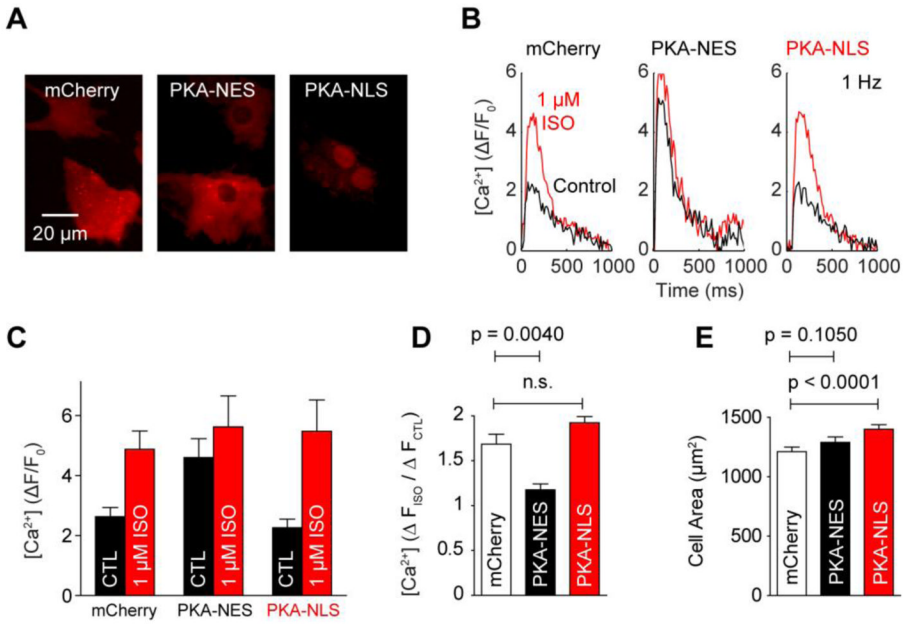

Fig. 7.

PKA compartmentation underlies selection of contractile and cell hypertrophic β-adrenergic signaling responses. A, Expression of mCherry, PKA-NES and PKA-NLS plasmids. B, Representative Fluo-4 Ca^{2+} responses to 1 μmol/L ISO for expressing cells under 1 Hz pacing. C, Mean Fluo-4 Ca^{2+} transients before and after stimulation by 1 μmol/L ISO ($n \geq 3$ experiments each). Baseline (Control: CTL) Fluo-4 Ca^{2+} transients are nearly saturated in PKA-NES myocytes. D, Mean enhancements to Fluo-4 Ca^{2+} transients by 1 μmol/L ISO stimulation. 1 μmol/L ISO elicits robust enhancements to mCherry and PKA-NLS myocytes, but not PKA-NES myocytes ($n > 3$ experiments each). E, Median cell size measurements in expressing cells. PKA-NLS induces hypertrophic growth in cell area, while PKA-NES does not ($n > 900$ cells each).